Co-published by
Institute of Fluid-Flow Machinery
Polish Academy of Sciences
Committee on Thermodynamics and Combustion
Polish Academy of Sciences

http://www.imp.gda.pl/archives-of-thermodynamics/

Effects of cooling methods and key parameters on the cooling performance of oil-cooling motor with hairpin windings

Y.X. Liu[ab*], H. Wu[b], J. Zhang[b], P.X. Xu[c], S. Chen[c], X.H. He[a], Z.D. Sun[d]

[a]School of Smart Health, Chongqing College of Electronic Engineering, Chongqing, 401331, China
[b]Department of Technology, Chongqing Tsingshan Industrial Co. Ltd., Chongqing, 402776, China
[c]College of Mechanical Engineering, Chongqing University of Technology, Chongqing 400044, China
[d]Hubei University of Automotive Technology, Shiyan Hubei, 442002, China
*Corresponding author: liugw215@126.com

Received: 11.12.2023; revised: 21.02.2024; accepted: 22.04.2024

Abstract

Based on the electromagnetic thermal coupling analysis method, the cooling performance of different motor cooling models and the influence of key parameters of the cooling system on the cooling effect of the motor are investigated. First, the losses of various parts of the permanent magnet synchronous motors are obtained through electromagnetic calculations; the analysis results show that the stator core loss, winding copper loss, and eddy current loss of permanent magnets exceed 95% of the total loss of the motor. Second, the cooling performance of the three motor was compared and analyzed. The axial housing liquid cooling and oil spray cooling (Model B) has a better cooling performance and a higher cooling efficiency. Compared with the other two motor models, Model B can reduce the time to reach steady-state temperature by about 81.8%.Then the effects of coolant volume flow rate, coolant inlet temperature, and ambient temperature on the cooling effect of the motor are investigated. The results show that within a certain range, the rate of coolant inlet temperature change is approximately proportional to the internal temperature rise of the motor. The oil spray cooling system of Model B is less affected by ambient temperature and can be used for motor cooling in complex environments. The results of this study can provide a useful guidance for the design of the cooling system and the selection of coolant volume flow rate for oil-cooling motor with hairpin windings.

Keywords: Hairpin winding; Electromagnetic-thermal coupling; Permanent magnet synchronous motors; Cooling performance; Oil spray cooling

Vol. 45(2024), No. 2, 301–309; doi: 10.24425/ather.2024.150874

Cite this manuscript as: Liu, Y.X., Wu, H., Zhang, J., Xu, P.X., Chen, S., He, X.H., & Sun Z.D. (2024). Effects of cooling methods and key parameters on the cooling performance of oil-cooling motor with hairpin windings. *Archives of Thermodynamics*, 45(2), 301−309.

1. Introduction

Due to fluctuations in fuel prices, emission restrictions, and increasing public awareness of global warming, electric vehicles (EVs) have been welcomed as the future of passenger car and light transport vehicle industry [1−2]. In this case, motors with high power density are needed to reduce weight and extending the travel range of EVs. Due to its ability to increase motor power density, hairpin windings are being increasingly adopted in EV drive motors and have become a research hotspot in recent years [3−5].

Permanent magnet synchronous motors (PMSM) is one of

Nomenclature

B_m – amplitude of the magnetic flux density, T
f – frequency, Hz
I – effective value of phase current pressure, A
k_c – additional locc coefficient,
k_e – eddy current loss coefficient,
k_h – hysteresis locc coefficient,
m – number of phases in the motor,
P_{AC1} – AC copper loss caused by skin effect, W
P_{AC2} – AC copper loss caused by proximity effect, W
P_c – additional loss, W
P_{Cu} – total winding loss of the motor, W
P_{DC} – DC copper loss, W
P_e – eddy current loss, W
P_h – hysteresis loss, W
P_{pm} − eddy current loss in permanent magnets, W
r – winding resistance, Ω

Greek symbols

σ − electrical conductivity, S/m

Abbreviations and Acronyms

AC − alternating current
DC − direct current
EV – electric vehicle
PMSM − permanent magnet synchronous motors

the most commonly used types of motors in the power transmission system of electric vehicles. The motor cooling method for a PMSM can be air cooling, water cooling, or oil cooling [6−8]. Although air cooling [9,10] and water jacket cooling [11,12] are widely used for thermal management of motors, they cannot meet the demanding requirements of higher heat flux in future motors due to the poor thermal conductivity of laminations and insulation materials. Modern EVs require the smallest weight to achieve high power, thereby increasing heat generation and reducing heat dissipation space [13]. The performance of motors is thus typically limited by their ability to remove heat from critical components, requiring an efficient cooling system [14]. To meet the cooling performance of high-power density motors, various advanced cooling methods and design concepts have been proposed. Lindh et al. [15] combined cooling tubes with the slot winding and tested its performance with three real drive cycles, the cooling capability was extremely promising, and the motors winding average temperature reaches only 77°C temperatures. Madonna et al. [16] developed a novel thermal management method, their modelling and experimental results show that a 25% hot-spot temperature reduction on a particular application can be achieved. Liu et al. [17] conducted experimental research on oil spray cooling for end winding and discussed the effects of spray parameters and nozzle structure, hot spots on end-windings can be expected within the top half, from the 10 o'clock to the 2 o'clock positions, and the cooling performances of full-cone nozzles are generally better than the hollow-cone nozzle. Wang et al. [18] have designed three kinds of novel PMSM integrated with heat pipe, the heat transfer performance between the heat pipe and the end cap is significantly improved compared to traditional PMSM cooling systems, the highest temperatures of the end winding are 149.9°C, 140.1°C, 133.5°C, and 139.6°C for the traditional PMSM and the three new PMSMs, respectively. Wang et al. [19] investigated a novel direct cooling structure for the primary core and windings, integrated with the advantage of a filler with high thermal conductivity, which can greatly reduce the thermal resistances between the heat source and the coolant and thus improves the cooling performance. Wang et al. [20] studied the thermal management of the end winding of oil spray and established a prediction model for heat transfer performance, the predicted results of the model coincided with experimental data very well with the MSE and correlation coefficient of 7.28 and 0.93, respectively. Guo et al. [21] proposed a novel hybrid cooling method for high-speed high-power permanent magnet assisted synchronous reluctance starter/generator, which can decrease 10% and 35.7% temperature compared with the cooling method of the oil circulation in the housing, oil spray at winding ends and the cooling method of the oil spray at rotor end surface. According to studying the oil spray cooling parameters of end windings [22], it was found that around 75% increase of the total heat transfer coefficient and 8 times decrease of the uniformness of wall temperature can be achieved by increasing around half the flow rate of the coolant liquid. Zhao et al. [23] proposed a water-cold plate cooling structure between the axial laminations of the motor stator. Compared with the outer spiral water jacket cooling structure, the maximum and average temperatures of the water-cooled plate structure were reduced by 25.5% and 30.5%, respectively. The thermal losses of PMSMs are primarily caused by mechanical, magnetic, copper losses and bearing friction losses [24]. Copper losses occur in the winding conductors and can be evaluated through Joule loss relation [25]. The mechanical losses are caused by friction between the rotor and air inside the air gap [26]. Magnetic loss or iron loss, including hysteresis and eddy current losses of the rotor and stator, can be estimated by constants related to motor material and electromagnetic configuration [27]. Due to many details often being unknown, significant errors often occur when using theoretical calculations to calculate the heat loss value of a motor. Therefore, modeling software and electromagnetic thermal calculation software are usually used for numerical evaluation, such as Altair Flux [28] or Ansys Motor-CAD [29].

Research on hairpin winding oil cooled motors mainly focuses on optimizing the cooling system. However, more comprehensive research is needed on the impact of key parameters of the cooling system on the cooling performance of the motor. On this basis, taking a PMSM with hairpin windings as the research object, a motor loss solution model was established based on the theory of electromagnetism and heat transfer. In addition, based on the electromagnetic thermal coupling analysis method, the cooling performance of different motor cooling models and the influence of key parameters of the cooling system on the cooling effect of the motor were investigated. The research results can provide a useful guidance for the design of cooling system and key parameters for PMSM with hairpin windings.

2. Material and method

2.1. Motor model and parameters

The research object is the permanent magnet synchronous drive motor for EVs, which adopts a hairpin winding. The axial structure and composition of the motor are shown in Fig. 1, and the basic parameters of the motor are shown in Table 1.

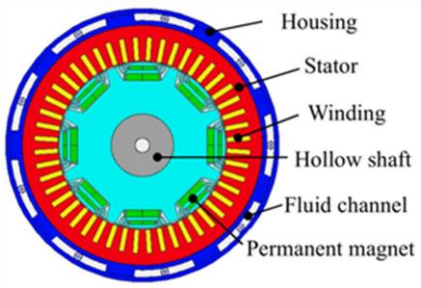

Fig. 1. PMSM with hairpin windings.

Table 1. Basic parameters of PMSM.

Parameters	Values
Rated speed (r/min)	6 000
Rated power (kW)	150
Number of stator slots	48
Pair of poles	8
Outer diameter of stator(mm)	250
Inner diameter of stator(mm)	175
Cooling method	Oil cooling
Number of winding layers	6
Coil type	Hairpin winding

To analyse the influence of different cooling systems on the cooling performance of the motor, three cooling models were created based on the prototype model (Fig. 1): axial housing liquid cooling model (Model A), axial housing liquid cooling and oil spray cooling model (Model B), and axial housing liquid cooling and hollow shaft cooling model (Model C). In Model A, there are 9 evenly distributed coolant flow channels along the circumference of the housing. The coolant enters from the front inlet of the motor and flows out from the rear outlet along the axial direction (see Fig. 3a). In addition, to better compare and analyse the cooling performance of the three different cooling systems, ATF134 coolant is selected, with a thermal conductivity of 0.1338 W/(m·K), a specific heat capacity of 2.26 J/(kg·K), and a density of 811.8 kg/m^3.

2.2. Losses analysis of motor with hairpin windings

1) Iron core loss

Iron core loss (referred to as iron loss) is a general term for power losses caused by hysteresis and eddy currents in the core during AC magnetic circuits. The iron loss inside the motor can be divided into three parts: eddy current loss, hysteresis loss and additional loss. Based on the Bertotti iron loss calculation model, the iron loss per unit mass can be express as follows [30]:

$$P_{\mathrm{Fe}} = P_h + P_c + P_e = k_h f B_m^2 + k_c f^2 B_m^2 + k_e f^{1.5} B_m^{1.5}, \quad (1)$$

where P_h is hysteresis loss, W; P_c is additional loss, W; P_e is eddy current loss, W; B_m is the amplitude of the magnetic flux density, T; f is the frequency, Hz; k_h, k_c and k_e are the hysteresis loss coefficient, additional loss coefficient and eddy current loss coefficient, respectively.

2) Winding copper loss

For conventional round wire motors, the AC copper loss during motor operation can be ignored. The total copper loss in the motor can be represented by the DC copper loss, which is proportional to the square of the current and the resistance. However, for hairpin winding motors, the skin effect and proximity effect in the windings are more significant, resulting in larger eddy current losses. Therefore, the copper loss in hairpin windings can be divided into three parts: DC copper loss, AC copper loss caused by skin effect, and AC copper loss caused by proximity effect:

$$P_{\mathrm{Cu}} = P_{\mathrm{DC}} + P_{\mathrm{AC1}} + P_{\mathrm{AC2}}\ , \quad (2)$$

where P_{Cu} is the total winding loss of the motor; P_{DC} is the DC copper loss; P_{AC1} is the AC copper loss caused by skin effect; P_{AC2} is the AC copper loss caused by proximity effect:

$$P_{\mathrm{DC}} = mI^2 r\ , \quad (3)$$

where m is the number of phases in the motor; I is the effective value of phase current; r is the winding resistance.

The factors that affect the copper loss of hairpin winding motors can be divided into two categories: winding structural parameters and winding energization parameters. In practical calculations, analytical calculation methods are often unable to accurately calculate the copper loss. Therefore, finite element simulation is commonly used to calculate the winding copper loss.

3) Eddy current loss in permanent magnets

During the actual operation of the motor, there are certain harmonic components in the air gap magnetic field. These harmonic components induce eddy currents within the permanent magnets, resulting in a certain eddy current loss. The loss can be calculated as follows [31]:

$$P_{pm} = \int_V^{\cdot} \delta E^2 \mathrm{d}V = \int_V^{\cdot} J^2/\sigma \mathrm{d}V, \quad (4)$$

where P_{pm} is the eddy current loss in permanent magnets, W; σ is the electrical conductivity, S/m; J is the eddy current density, W/m^3; E is the electric field strength, N/C, and V is the spatial integration area.

3. Results and discussion

3.1. Motor loss calculation

During the operation of a PMSM, due to electromagnetic and mechanical losses, its internal components will convert electrical energy into thermal energy, resulting in an increase in motor

temperature. The electromagnetic-thermal coupling method allows the motor losses obtained from electromagnetic calculations to be directly input into the temperature field calculation of the motor. In the calculation process, the heat transfer between the various components of the motor mainly occurs through conduction and convection, while the influence of thermal radiation between the components is ignored. To simplify the analysis, the following assumptions are made in the electromagnetic thermal coupling calculation:

1) the influence of heat dissipation from the motor end cover on the motor temperature is ignored, and only the heat transfer between the motor housing and the external air is considered,
2) only conduction and convection are considered between the various components and between the components and the air or cooling liquid,
3) the variation in thermal conductivity, heat transfer coefficient, and heat transfer coefficient within the motor due to temperature changes are ignored,
4) the insulation material of the winding is uniformly distributed, and the thermal conductivity between the different parts is consistent.

Based on the above assumptions, the losses of each component of the PMSM with hairpin windings under rated operating conditions can be obtained through electromagnetic calculations, as shown in Table 2.

Table 2. Motor losses under rated operating conditions (W).

Name	Stator iron loss	DC copper loss	Rotor iron loss	Eddy current loss of magnet
Loss value	710.6	2 529	107.4	64.98

From the calculation results, it can be seen that the stator iron core losses, winding copper losses and permanent magnet eddy current losses account for over 95% of the total motor losses.

3.2. Temperature characteristics of housing axial liquid cooling

To compare and analyse the influence of the cooling system on the temperature field distribution of the motor, the temperature field distribution of the housing axial cooling model (Model A) is calculated first based on the electromagnetic thermal coupling method. During the analysis, the coolant volume flow rate, inlet temperature, and ambient temperature are set as10 L/min, 65°C, and 40°C, respectively. Due to the axial symmetry of the studied motor model, half of the motor model A is taken as the research object. Through calculation, it can be concluded that under rated operating conditions, the steady-state temperature distribution along the axial direction of Model A is shown in Fig. 2a, and the relationships between the transient temperature and time of each component is shown in Fig. 2b. It can be seen from Fig. 2a that the highest temperature inside the motor is found in the end winding, with a steady-state temperature of 213.91°C, and the steady-state temperatures of the stator core and permanent magnet are 195.74°C and 195.01°C, respectively. It can be observed from Fig. 2b that the transient temperatures of different components of the motor increase overtime. After approximately 3 000 s, the temperature increase rate of the winding and stator iron core gradually decreases. The temperatures of the permanent magnet, rotor and shaft gradually reach a steady-state stage after about 5 000 s. The above analysis results indicate that for housing liquid-cooled motors, the temperature rise of the winding, stator core, and permanent magnet is relatively large, and they are the main heat source for the internal temperature rise of the motor. In addition, for the housing liquid-cooled motor, during operation, the temperature of the stator and winding in direct contact with the housing reaches a steady-state stage first.

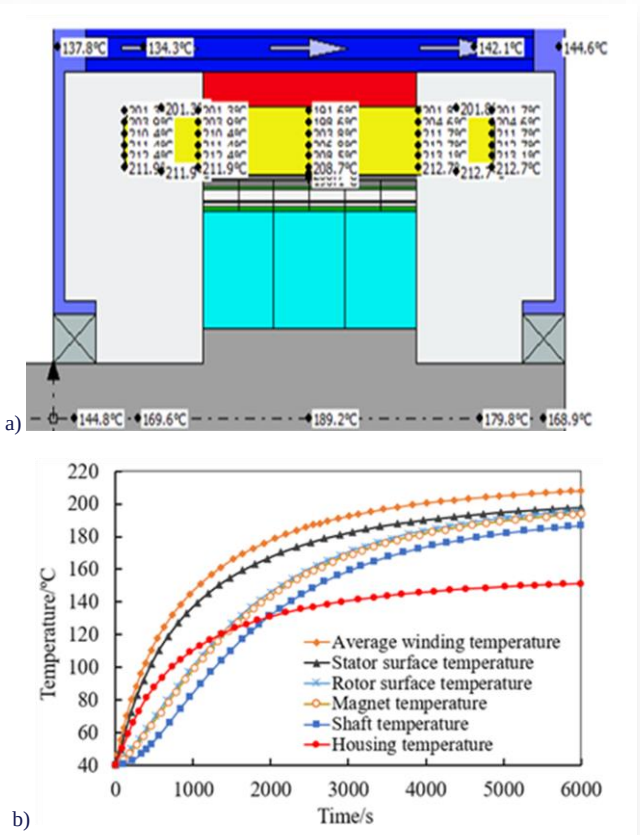

Fig. 2. Steady state temperature distribution and transient temperature variation curve of Model A: a) the steady-state temperature distribution along the axial direction, b) the relationships between the transient temperature of the motor and time.

The operating temperature of neodymium iron boron magnets in PMSM should generally not exceed 200°C. The maximum temperature of the stator and rotor iron cores should not exceed 250°C, and the maximum operating temperature of the shaft is 200°C. When the temperature is too high, irreversible demagnetization can occur in the permanent magnet, and excessive temperatures in the stator and rotor iron cores can lead to insulation layer damage, increased iron losses, and decreased mechanical strength. The insulation class of the motor here is Class H, with a maximum allowable temperature for the stator winding of 180°C and a reference temperature of 145°C. Therefore, for the hairpin winding motor in this study, using only liq

uid cooling in the housing is not sufficient to maintain the temperature rise within an acceptable limit, and the motor will not be able to operate normally. Hence, further optimization of the cooling system is necessary to control the temperature of the permanent magnet below 180°C and the temperature of the stator winding below the reference temperature of 145°C.

3.3. Impact of cooling system on cooling performance

This section mainly compares and analyses the structural characteristics and cooling performance of three cooling systems: Model A, Model B, and Model C. According to the calculation results of the steady-state and transient temperatures of components in Model A (Fig. 1), it can be seen that the average temperature of the windings, the surface temperature of the stator core, and the temperature of the permanent magnets vary significantly during motor operation. When comparing the three models, the focus is on studying the variation of the average temperature of the windings, the surface temperature of the stator core, and the temperature of the permanent magnets under the same boundary conditions, as well as the cooling performance of the three different cooling systems.

The structures of the three motor cooling models are shown in Fig. 3.

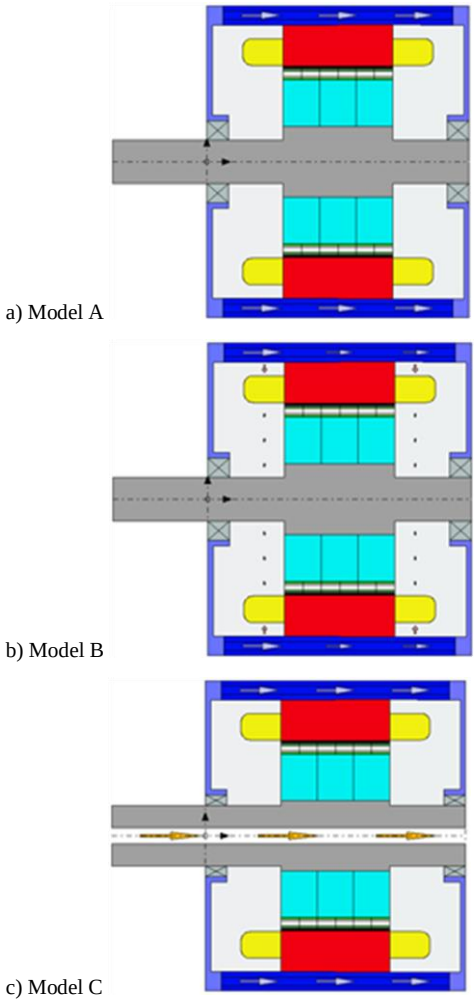

Fig. 3. Structure comparison of three cooling models.

An axial oil channel is used in Model A, where the coolant flows along the axial direction in the housing (the arrow indicates the direction of coolant flow (Fig. 3a). Model B (Fig. 3b) has ring-shaped oil grooves arranged at the front and rear end windings, with 16 oil spray holes evenly distributed on the grooves. The oil sprayed from the spray holes fall onto the shaft, and under the action of centrifugal force, some of the coolant is thrown onto the end windings, enhancing the cooling effect of the end windings. Model B and Model C (Fig. 3c) are two cooling models based on the structural optimization of Model A. The cooling structure of the housing of Model C is the same as that of Model A, and in addition, a hollow shaft cooling is added. The coolant flows from the front end of the hollow shaft to the rear end. The structural parameters of the axial oil passage in the motor housing for the three models are the same. The key structural parameters of Model B and Model C are shown in Table 1.

The main parameter settings for steady-state temperature rise calculation in the three motor models are as follows: the coolant inlet flow rate is 10 L/min; the inlet temperature is 65°C; the ambient temperature is 40°C, and the rated speed is 6 000 r/min. The internal coolant volume flow rate of the shaft in Model C is 2 L/min. The steady-state temperatures of typical components in the three motor models are shown in Fig. 4. From the results of Fig. 4, it can be visually seen that Model B has the best cooling performance, with a steady-state temperature rises of 126.44°C, 119.79°C, and 79.69°C for the windings, stator core and permanent magnets, respectively. Compared with Model A, the steady-state temperature of the windings and the steady-state temperature of the permanent magnets in Model B decrease by 38.19% and 58.55%, respectively. Therefore, based on the above analysis results, it can be concluded that among the three motor cooling models, Model B has better cooling performance because the coolant in Model B can directly contact the internal components of the motor, quickly absorbing their heat.

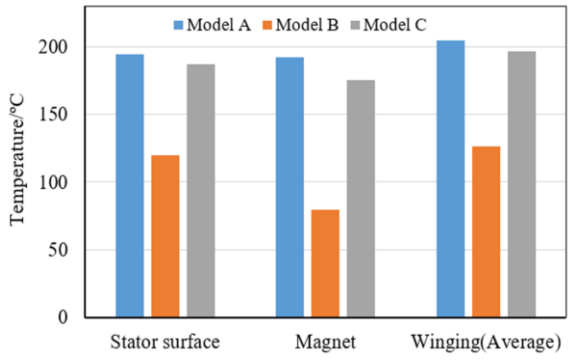

Fig. 4. Steady-state temperatures of typical components in three motor models.

Figure 4 presents the steady-state temperatures of typical components in the three motor models. To more accurately evaluate the cooling performance of different motor models, transient temperature calculations are performed on the motor. In the calculation process, the parameter settings for coolant volume flow rate, inlet temperature, and ambient temperature are the

same as those for steady-state calculations. Under rated operating conditions, the transient temperature variation curves of the windings and permanent magnets in the three motor cooling models are shown in Fig. 5. From the transient temperature analysis results of the three models, it can be observed that after approximately 1 000 seconds of motor operation, the average winding temperature and permanent magnet temperature of Model B tend to stabilize and enter a stable state. The average winding temperature and permanent magnet temperature of Model A and Model C tend to stabilize after about 5 500 seconds of motor operation. It can be seen from the transient temperature changes of the three motor models that the internal temperature of Model B is significantly lower than that of the other two models. The above analysis results indicates that among the three motor cooling models, the oil spray cooling in Model B can achieve fast cooling of various components of the motor, with a higher cooling rate. Compared with the other two motor cooling models, Model B can reduce the time to reach steady-state temperature by about 81.8%. Additionally, due to the presence of an oil spray cooling system, the winding temperature at the end is slightly lower than that of the winding inside the slots.

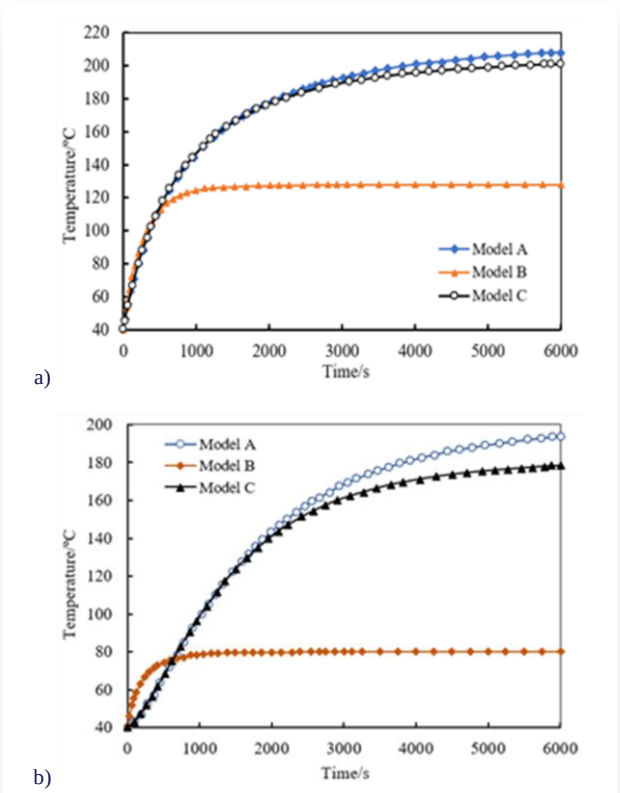

Fig. 5. Transient temperature variation curve with time: a) average winding temperature,(b) permanent magnet temperature.

3.4. Effect of coolant volume flow rate on cooling performance

The magnitude of the coolant flow rate directly determines the selection of the coolant pump. A scientifically and reasonably chosen coolant pump can reduce energy consumption and also contribute to weight and cost reduction. Therefore, it is necessary to conduct a systematic study on the volume flow rate of the coolant inlet. According to comparing and analyzing the motor temperature characteristics of the three cooling systems, the influence of coolant volume flow rate on steady-state temperature reduction in the motor was investigated. All three motor cooling models use ATF134 as the cooling medium, with a coolant inlet temperature of 65°C. The influence of coolant volume flow rate on internal motor temperature can be obtained through calculations, as shown in Fig. 6.

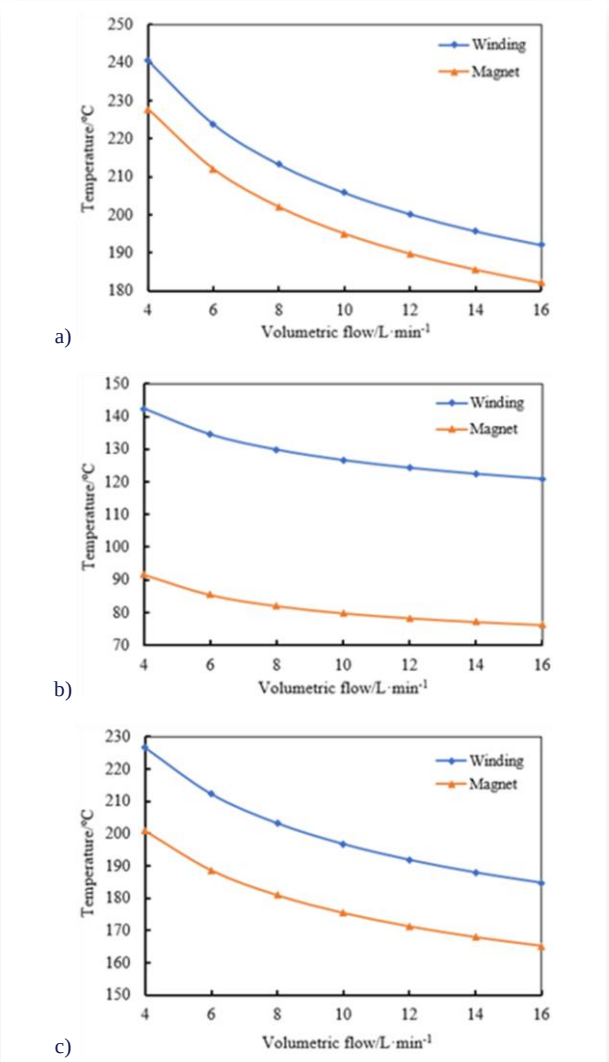

Fig. 6. Relationships between steady-state temperature of different cooling systems and coolant volume flow rate: a) Model A, b) Model B, c) Model C.

From the analysis results in Fig. 6, it can be seen that:

1) As the coolant volume flow rate changes, the temperature of the stator winding is consistently higher than that of the permanent magnets. When designing the motor cooling system, special attention should be paid to the temperature of the stator winding;
2) For Model B, a coolant flow rate of 6 L/min can meet the performance temperature allowance for Class H, with good economy. However, Model A and Model C require a larger coolant volume flow rate;
3) With the same coolant volume flow rate, oil spray cooling can significantly reduce the motor temperature;

4) The relationship between coolant flow rate and motor temperature is nonlinear. When the coolant flow rate increases to a certain value, the influence of coolant flow rate on motor temperature gradually decreases. These findings provide a valuable guidance for selecting the coolant volume flow rate for motor cooling.

3.5. Effect of coolant inlet temperature on cooling performance

At a coolant flow rate of 10 L/min and an ambient temperature of 40°C, the variation of the temperature field of the three motors is investigated as the coolant inlet temperature changes from 40°C to 80°C. The calculated results are shown in Fig. 7.

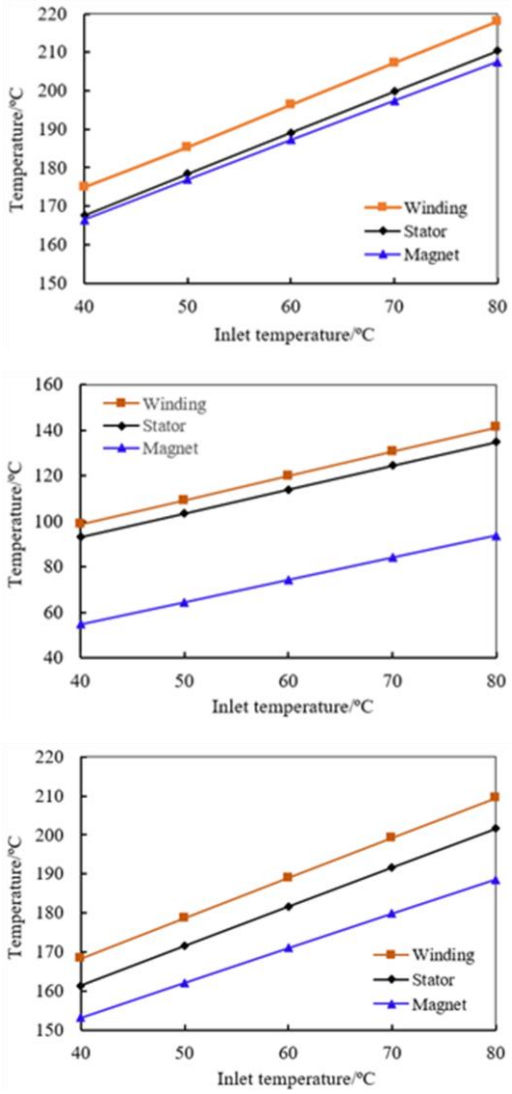

Fig. 7. The relationship between the internal temperature of motor and the inlet temperature of the coolant.

From the analysis results, it can be seen that the rate of change of coolant inlet temperature is directly proportional to the internal temperature rise of the motor, meaning that a higher inlet temperature results in a higher internal temperature of the motor. As the inlet temperature increases, the internal temperature rise of Model B exhibits greater variation compared to the other models. Under the same coolant inlet temperature, the internal temperature of the motor shows more pronounced changes. For Model B, for every 1°C increase in coolant inlet temperature, the stator winding temperature increases by approximately 1.076°C, and the permanent magnet temperature increases by approximately 0.984°C. The above analysis indicates that the coolant inlet temperature directly affects the temperature rise inside the motor. During the design process of the motor cooling system, reducing the coolant inlet temperature can effectively lower the internal temperature of the motor.

3.6. Effect of ambient temperature on cooling performance

This section investigates the variations in the steady-state temperature field of three types of motors as the ambient temperature fluctuates between 20°C and 60°C. The impact of ambient temperature on the steady-state temperature rise of key components of the motor is shown in Fig. 8.

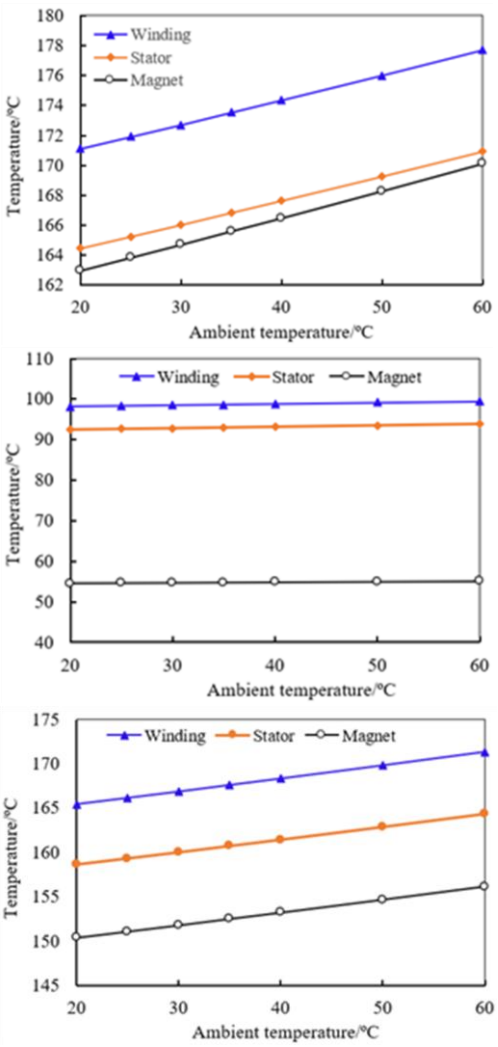

Fig. 8. The relationship between the internal temperature of motor and ambient temperature.

The main parameters used in the calculations are a coolant flow rate of 10 L/min, a coolant inlet temperature of 40°C, and an inner coolant volume flow rate of 2 L/min. From the analysis results, it can be seen that in Model A and Model C, as the ambient temperature increases, the temperature of each internal component of the motor tends to rise, and the degree of influence varies among different components. In Model B, however, the temperatures of the internal components hardly change with increasing ambient temperature.

These analysis results indicate that the different motor cooling systems are affected to varying degrees by the ambient temperature. The spray cooling system in Model B is less affected by the ambient temperature and can be used for motor cooling in complex environments.

4. Conclusions

A PMSM with hairpin windings is investigated in this paper. The influences of key parameters of the cooling system on motor cooling performance are studied based on the electromagnetic-thermal coupling analysis method. The following conclusions are drawn:

1) The thermal losses of the PMSM with hairpin windings primarily originate from the stator iron core and the copper losses in the windings. The permanent magnet eddy current loss accounts for more than 95% of the total motor losses, making it the primary heat sources within the motor.
2) The Model B has the best cooling performance in the three models. Compared with the other two motor models, the steady-state temperature of Model B's winding and permanent magnet is decreased by 38.19% and 58.55%, respectively, and the time to reach steady-state temperature also decreased by about 81.8%.
3) The coolant flow rate and temperature in the motor exhibits a non-linear relationship. For Model B, when the coolant flow rate is greater than 6 L/min, the temperature change inside the motor is relatively small and the economy is weakened.
4) The coolant inlet temperature has an impact on the cooling performance of the motor. For the three studied motor models, the rate of change of the coolant inlet temperature is directly proportional to the internal temperature rise of the motor.
5) The oil spray cooling system in Model B is less influenced by the ambient temperature, making it suitable for motor cooling in complex environments. For models A and C, as the ambient temperature increases, the internal temperature of the motor significantly increases. However, in Model B, the temperature of the internal components hardly changes as the ambient temperature increase.

Acknowledgements

This work was supported by the Natural Science Foundation of Chongqing (Grant No.: CSTB2023NSCQ-MSX0255), and Science and Technology Research Program of Chongqing Municipal Education Commission (Grant No.: KJQN202203110 and KJZD-K202203404).

References

[1] Kumar, A., Chandekar, A., Deshmukh, P.W., & Ugale, R.T. (2023). Development of electric vehicle with permanent magnet synchronous motor and its analysis with drive cycles in MATLAB/Simulink. *Materials Today: Proceedings*, 72, 643−651. doi: 10.1016/j.matpr.2022.08.304

[2] Gammaidoni, T., Zembi, J., Battistoni, M., Biscontini, G., & Mariani, A. (2023). CFD analysis of an electric motor's cooling system: Model validation and solutions for optimization. *Case Studies in Thermal Engineering*, 49, 103349. doi: 10.1016/j.csite.2023.103349

[3] Ha, T., & Kim, D.K. (2021). Study of injection method for maximizing oil-cooling performance of electric vehicle motor with hairpin winding. *Energies*, 14(3), 747. doi: 10.3390/en14030747

[4] Zhang, F., Gerada, D., Xu, Z., Liu, C., Zhang, H., Zou, T., Chong, Y.C., & Gerada, C. (2021). A thermal modeling approach and experimental validation for an oil spray-cooled hairpin winding machine. *IEEE Transactions on Transportation Electrification*, 7(4), 2914–2926. doi: 10.1109/tte.2021.3067601

[5] Ha, T., Kang, Y., Kim, N.S., Park, S.H., Lee, S.H., Kim, D.K., & Ryou, H.S. (2021). Cooling effect of oil cooling method on electric vehicle motors with hairpin winding. *Journal of Mechanical Science and Technology*, 35(1), 407–415. doi: 10.1007/s12206-020-1240-y

[6] Gai, Y., Kimiabeigi, M., Chuan Chong, Y., Widmer, J.D., Deng, X., Popescu, M., Goss, J., Staton, D.A., & Steven, A. (2019). Cooling of automotive traction motors: Schemes, examples, and computation methods. *IEEE Transactions on Industrial Electronics*, 66(3), 1681–1692. doi: 10.1109/tie.2018.2835397

[7] Carriero, A., Locatelli, M., Ramakrishnan, K., Mastinu, G., & Gobbi, M. (2018). A review of the state of the art of electric traction motors cooling techniques. *SAE Technical Paper*, 2018-01-0057. doi: 10.4271/2018-01-0057

[8] Liange, H., Hongling, C., & Wenjun, S. (2022). Erratum to "Boiling heat transfer-based temperature rise characteristics of automotive permanent magnet synchronous motors at peak operating conditions". *Journal of Mechanical Science and Technology*, 36(8), 4335–4335. doi: 10.1007/s12206-022-0750-1

[9] Ulbrich, S., Kopte, J., & Proske, J. (2018). Cooling fin optimization on a TEFC electrical machine housing using a 2-D conjugate heat transfer model. IEEE *Transactions on Industrial Electronics (1982)*, 65(2), 1711–1718. doi: 10.1109/tie.2017.2748051

[10] Peng, H.S., & Lai, F.H. (2019). Investigation of parameters affecting heat transfer and fluid flow of a TEFC electric motor by using Taguchi method. *IOP Conference Series. Materials Science and Engineering*, 491, 012021. doi: 10.1088/1757-899x/491/1/012021

[11] Li, J., Lu, Y., Cho, Y.H., & Qu, R. (2019). Design, analysis, and prototyping of a water-cooled axial-flux permanent-magnet machine for large-power direct-driven applications. *IEEE Transactions on Industry Applications*, 55(4), 3555–3565. doi: 10.1109/tia.2019.2907890

[12] Wu, P.S., Hsieh, M.F., Cai, W.L., Liu, J.H., Huang, Y.T., Caceres, J.F., & Chang, S.W. (2019). Heat transfer and thermal management of interior permanent magnet synchronous electric motor. *Inventions*, 4(4), 69. doi: 10.3390/inventions4040069

[13] Li, Y., Li, Q., Fan, T., & Wen, X. (2023). Heat dissipation design of end winding of permanent magnet synchronous motor for electric vehicle. *Energy Reports*, 9, 282–288. doi: 10.1016/j.egyr.2022.10.416

[14] Gai, Y., Ma, C., Xu, Y., & Chong, Y.C. (2021). Numerical prediction and measurement of pressure drop and heat transfer in

a water-cooled hollow-shaft rotor for a traction motor application. *IET Electric Power Applications*, 15(4), 476–486. doi: 10.1049/elp2.12042

[15] Lindh, P., Petrov, I., Pyrhonen, J., Scherman, E., Niemela, M., & Immonen, P. (2019). Direct liquid cooling method verified with a permanent-magnet traction motor in a bus. *IEEE Transactions on Industry Applications*, 55(4), 4183–4191. doi: 10.1109/tia.2019.2908801

[16] Madonna, V., Walker, A., Giangrande, P., Serra, G., Gerada, C., & Galea, M. (2019). Improved thermal management and analysis for Stator end-windings of electrical machines. *IEEE Transactions on Industrial Electronics (1982)*, 66(7), 5057–5069. doi: 10.1109/tie.2018.2868288

[17] Liu, C., Xu, Z., Gerada, D., Li, J., Gerada, C., Chong, Y.C., Popescu, M., Goss, J., Staton, D., & Zhang, H. (2020). Experimental investigation on oil spray cooling with hairpin windings. *IEEE Transactions on Industrial Electronics (1982)*, 67(9), 7343–7353. doi: 10.1109/tie.2019.2942563

[18] Wang, X., Wan, Z., & Wen, W. (2021). Heat dissipation of three permanent magnet synchronous motors integrated with heat pipes. *International Journal of Thermophysics*, 42(5). doi: 10.1007/s10765-021-02819-8

[19] Wang, Z., Huang, X., & Liu, J. (2023). Comparative investigation and optimization of a direct cooling structure for the primary core and windings in permanent magnet synchronous linear motors. *Applied Thermal Engineering*, 228, 120499. doi: 10.1016/j.applthermaleng.2023.120499

[20] Wang, X., Li, B., Huang, K., Yan, Y., Stone, I., & Worrall, S. (2022). Experimental investigation on end winding thermal management with oil spray in electric vehicles. *Case Studies in Thermal Engineering*, 35, 102082. doi: 10.1016/j.csite.2022.102082

[21] Guo, H., He, X., Xu, J., Tian, W., Ding, X., Ju, L., & Li, D. (2023). Design and analysis of a novel hybrid cooling method of high-speed high-power permanent magnet assisted synchronous reluctance starter/generator in aviation applications. *Chinese Journal of Aeronautics*, 36(3), 285–302. doi: 10.1016/j.cja.2022.08.017

[22] Zhao, A., Duwig, C., Liu, C., Gerada, D., & Leksell, M. (2023). Parameter study for oil spray cooling on end windings of electric machines via Eulerian–Lagrangian simulation. *Applied Thermal Engineering*, 235, 121281. doi: 10.1016/j.applthermaleng.2023.121281

[23] Zhao, X., Cui, H., Teng, Y., Chen, Z., & Liu, G. (2023). Design and analysis of a high loss density motor cooling system with water cold plates. *Global Energy Interconnection*, 6(3), 343–354. doi: 10.1016/j.gloei.2023.06.008

[24] Gundabattini, E., Kuppan, R., Solomon, D.G., Kalam, A., Kothari, D.P., & Abu Bakar, R. (2021). A review on methods of finding losses and cooling methods to increase efficiency of electric machines. *Ain Shams Engineering Journal*, 12(1), 497–505. doi: 10.1016/j.asej.2020.08.014

[25] Zhang, Y., Wang, L., Zhang, Y., & Zhang, Y. (2021). Design and thermal characteristic analysis of motorized spindle cooling system. *Advances in Mechanical Engineering*, 13(5), 168781402110208. doi: 10.1177/16878140211020878

[26] Bossmanns, B., & Tu, J.F. (1999). A thermal model for high speed motorized spindles. *International Journal of Machine Tools and Manufacture*, 39(9), 1345–1366. doi: 10.1016/s0890-6955(99)00005-x

[27] Madhavan, S., Devdatta, R., Gundabattini, E., & Mystkowski, A. (2022). Thermal analysis and heat management strategies for an induction motor, a review. *Energies*, 15(21), 8127. doi: 10.3390/en15218127

[28] Credo, A., Tursini, M., Villani, M., Di Lodovico, C., Orlando, M., & Frattari, F. (2021). Axial flux PM in-wheel motor for electric Vehicles: 3D multiphysics analysis. *Energies*, 14(8), 2107. doi: 10.3390/en14082107

[29] Jie, D. (2019). Thermal performance analysis of motor based on motor-CAD. *AIP Conference Proceedings*, 2073(1), 020049. *3rd International Conference on Advances in Materials, Machinery, Electronics*, 19−20 January, Wuhan, China. doi: 10.1063/1.5090703

[30] Xie, Y., Fan, Y., Cai, W., & Xin, W. (2023). Oil circuit structure optimization design and temperature field calculation of oil cooled motor with hairpin winding. *Electric Machines and Control*, 27, 37–45. doi: 10.15938/j.emc.2023.05.005

[31] Wang, C., Zhang, Z., & Liu, Y. (2021). Optimization of rotor eddy-current loss and heat dissipation for high torque density hybrid excitation synchronous motor with magnetic shunting rotor. *Proceedings of the of the Chinese Society of Electrical Engineering*, 41(21), 7476–7486 (in Chinese). doi: 10.13334/j.0258-8013.pcsee.201100